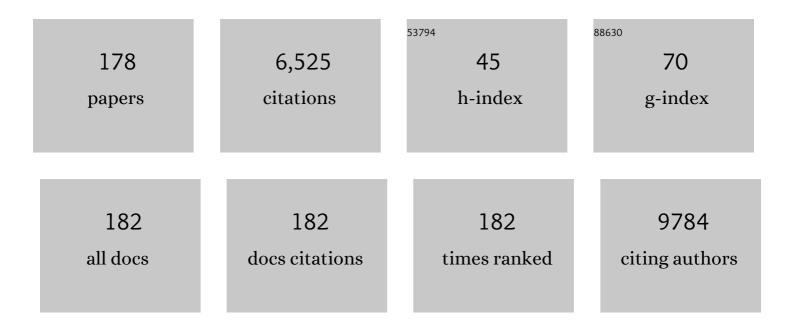
## **Chun Cheng**

List of Publications by Year in descending order

Source: https://exaly.com/author-pdf/467249/publications.pdf Version: 2024-02-01



#	Article	IF	CITATIONS
1	Nobleâ€Metalâ€Free Oxygen Evolution Reaction Electrocatalysts Working at High Current Densities over 1000 <scp>mA</scp> cm <sup>â°2</sup> : From Fundamental Understanding to Design Principles. En and Environmental Materials, 2023, 6, .	erg¥2.8	12
2	Sandwiched Li plating between Lithiophilic-Lithiophobic gradient Silver@Fullerene interphase layer for ultrastable lithium metal anodes. Chemical Engineering Journal, 2022, 429, 132156.	12.7	36
3	Intuitionistic fuzzy set of Γâ€submodules and its application in modeling spread of viral diseases, mutated COVID― <i>n</i> , via flights. International Journal of Intelligent Systems, 2022, 37, 5134-5151.	5.7	1
4	Organic Semiconductor–Insulator Blends for Organic Field‣ffect Transistors. Physica Status Solidi - Rapid Research Letters, 2022, 16, .	2.4	2
5	Bridging the gap between atomically thin semiconductors and metal leads. Nature Communications, 2022, 13, 1777.	12.8	17
6	Highly Orientational Order Perovskite Induced by In situâ€generated 1D Perovskitoid for Efficient and Stable Printable Photovoltaics. Small, 2022, 18, e2200130.	10.0	10
7	Doping Free and Amorphous NiO <sub>x</sub> Film via UV Irradiation for Efficient Inverted Perovskite Solar Cells. Advanced Science, 2022, 9, e2201543.	11.2	23
8	Soft hypergraph for modeling global interactions via social media networks. Expert Systems With Applications, 2022, 203, 117466.	7.6	6
9	Bridging the Interfacial Contact for Improved Stability and Efficiency of Inverted Perovskite Solar Cells. Small, 2022, 18, e2201694.	10.0	16
10	Construction of highly efficient Z-scheme ZnxCd1-xS/Au@g-C3N4 ternary heterojunction composite for visible-light-driven photocatalytic reduction of CO2 to solar fuel. Applied Catalysis B: Environmental, 2021, 282, 119600.	20.2	129
11	Rational construction of plasmonic Z-scheme Ag-ZnO-CeO2 heterostructures for highly enhanced solar photocatalytic H2 evolution. Applied Surface Science, 2021, 541, 148457.	6.1	39
12	Magnetic AgNPs/Fe <sub>3</sub> O <sub>4</sub> @chitosan/PVA nanocatalyst for fast one-pot green synthesis of propargylamine and triazole derivatives. New Journal of Chemistry, 2021, 45, 16119-16130.	2.8	15
13	Boosting the performance of MA-free inverted perovskite solar cells <i>via</i> multifunctional ion liquid. Journal of Materials Chemistry A, 2021, 9, 12746-12754.	10.3	44
14	Recent progress on kinetic control of chemical vapor deposition growth of high-quality wafer-scale transition metal dichalcogenides. Nanoscale Advances, 2021, 3, 3430-3440.	4.6	16
15	Strained Epitaxy of Monolayer Transition Metal Dichalcogenides for Wrinkle Arrays. ACS Nano, 2021, 15, 6633-6644.	14.6	37
16	Fully Optically Tunable and Flexible Composite Films for Enhanced Terahertz Control and Multifunctional Terahertz Devices. ACS Applied Electronic Materials, 2021, 3, 3044-3051.	4.3	12
17	Highly-Efficient Sulfonated UiO-66(Zr) Optical Fiber for Rapid Detection of Trace Levels of Pb2+. International Journal of Molecular Sciences, 2021, 22, 6053.	4.1	13
18	Phase Transition Hysteresis of Tungsten Doped VO <sub>2</sub> Synergistically Boosts the Function of Smart Windows in Ambient Conditions. ACS Applied Electronic Materials, 2021, 3, 3648-3656.	4.3	18

#	Article	IF	CITATIONS
19	NiCoS <i><sub>x</sub></i> @Cobalt Carbonate Hydroxide Obtained by Surface Sulfurization for Efficient and Stable Hydrogen Evolution at Large Current Densities. ACS Applied Materials & Interfaces, 2021, 13, 35647-35656.	8.0	23
20	Phase management in single-crystalline vanadium dioxide beams. Nature Communications, 2021, 12, 4214.	12.8	31
21	Research progress on graphene-based materials for high-performance lithium-metal batteries. New Carbon Materials, 2021, 36, 711-728.	6.1	26
22	Remarkable-cycling-performance anode for Li-ion battery: The bilayer β-bismuthene. Electrochimica Acta, 2021, 388, 138641.	5.2	7
23	Fundamental relations and identities of fuzzy hyperalgebras. Journal of Intelligent and Fuzzy Systems, 2021, 41, 2265-2274.	1.4	1
24	Antisolvent Engineering to Optimize Grain Crystallinity and Holeâ€Blocking Capability of Perovskite Films for Highâ€Performance Photovoltaics. Advanced Materials, 2021, 33, e2102816.	21.0	61
25	Vanadium dioxide for thermochromic smart windows in ambient conditions. Materials Today Energy, 2021, 21, 100827.	4.7	22
26	Facile fabrication of PVB-PVA blend polymer nanocomposite for simultaneous removal of heavy metal ions from aqueous solutions: Kinetic, equilibrium, reusability and adsorption mechanism. Journal of Environmental Chemical Engineering, 2021, 9, 106214.	6.7	33
27	Limitations and solutions for achieving high-performance perovskite tandem photovoltaics. Nano Energy, 2021, 88, 106219.	16.0	20
28	lon modification of transition cobalt oxide by soaking strategy for enhanced water splitting. Chemical Engineering Journal, 2021, 423, 130218.	12.7	24
29	Hierarchical CoP@Ni2P catalysts for pH-universal hydrogen evolution at high current density. Applied Catalysis B: Environmental, 2021, 296, 120350.	20.2	65
30	Boosting charge and thermal transport – role of insulators in stable and efficient n-type polymer transistors. Journal of Materials Chemistry C, 2021, 9, 12281-12290.	5.5	5
31	Quantitative Evaluation of Thermal Conductivity of Singleâ€Bent Microwire Using Vanadium Dioxide Temperature Tag. Physica Status Solidi (A) Applications and Materials Science, 2021, 218, 2100348.	1.8	1
32	Synthesis of Nanostructured Boron Nitride Aerogels by Rapid Pyrolysis of Melamine Diborate Aerogels via Induction Heating: From Composition Adjustment to Property Studies. ACS Applied Nano Materials, 2021, 4, 13788-13797.	5.0	8
33	Natural vs. Synthetic Phosphate as Efficient Heterogeneous Compounds for Synthesis of Quinoxalines. International Journal of Molecular Sciences, 2021, 22, 13665.	4.1	3
34	Physical and chemical reaction sensing in a mixed aqueous solution via metalâ€organic framework thinâ€film coated optical fiber. Microwave and Optical Technology Letters, 2020, 62, 72-77.	1.4	3
35	Electron Transporting Bilayer of SnO <sub>2</sub> and TiO <sub>2</sub> Nanocolloid Enables Highly Efficient Planar Perovskite Solar Cells. Solar Rrl, 2020, 4, 1900331.	5.8	46
36	Electron Transporting Bilayer of SnO <sub>2</sub> and TiO <sub>2</sub> Nanocolloid Enables Highly Efficient Planar Perovskite Solar Cells. Solar Rrl, 2020, 4, 2070014.	5.8	3

#	Article	IF	CITATIONS
37	Impact of Nanoscale Roughness on Heat Transport across the Solid–Solid Interface. Advanced Materials Interfaces, 2020, 7, 1901582.	3.7	24
38	Novel Sr5(PO4)2SiO4-graphene nanocomposites for applications in bone regeneration in vitro. Applied Surface Science, 2020, 507, 145176.	6.1	10
39	CeO <sub>2</sub> Nanostructures Enriched with Oxygen Vacancies for Photocatalytic CO <sub>2</sub> Reduction. ACS Applied Nano Materials, 2020, 3, 138-148.	5.0	148
40	Approaching optimal hole transport layers by an organic monomolecular strategy for efficient inverted perovskite solar cells. Journal of Materials Chemistry A, 2020, 8, 16560-16569.	10.3	16
41	Graphene oxide and its derivatives as promising In-vitro bio-imaging platforms. Scientific Reports, 2020, 10, 18052.	3.3	48
42	Low-temperature wafer-scale fabrication of vertical VO2 nanowire arrays. Applied Physics Letters, 2020, 117, .	3.3	7
43	Highly Efficient Visibleâ€Lightâ€Driven Photocatalytic Hydrogen Production Using Robust Nobleâ€Metalâ€Free Zn 0.5 Cd 0.5 S@Graphene Composites Decorated with MoS 2 Nanosheets. Advanced Materials Interfaces, 2020, 7, 2000010.	3.7	21
44	Novel versatile 3D bio-scaffold made of natural biocompatible hagfish exudate for tissue growth and organoid modeling. International Journal of Biological Macromolecules, 2020, 158, 894-902.	7.5	11
45	Multistimuliâ€Responsive Insectâ€Scale Soft Robotics Based on Anisotropic Superâ€Aligned VO <sub>2</sub> Nanowire/Carbon Nanotube Bimorph Actuators. Advanced Intelligent Systems, 2020, 2, 2000051.	6.1	14
46	Freestanding agaric-like molybdenum carbide/graphene/N-doped carbon foam as effective polysulfide anchor and catalyst for high performance lithium sulfur batteries. Energy Storage Materials, 2020, 33, 73-81.	18.0	81
47	Oxide Inhibitor-Assisted Growth of Single-Layer Molybdenum Dichalcogenides (MoX <sub>2</sub> , X =) Tj ETQq1	1 1 0.7843 14.6	314 rgBT /O
48	Black phosphorus-based van der Waals heterostructures for mid-infrared light-emission applications. Light: Science and Applications, 2020, 9, 114.	16.6	100
49	Multiple Regulation over Growth Direction, Band Structure, and Dimension of Monolayer WS <sub>2</sub> by a Quartz Substrate. Chemistry of Materials, 2020, 32, 2508-2517.	6.7	21
50	Simplified Compact Perovskite Solar Cells with Efficiency of 19.6% via Interface Engineering. Energy and Environmental Materials, 2020, 3, 5-11.	12.8	10
51	Hydroiodic Acid Additive Enhanced the Performance and Stability of PbS-QDs Solar Cells via Suppressing Hydroxyl Ligand. Nano-Micro Letters, 2020, 12, 37.	27.0	35
52	Approaching the Most Economic Preparation of Hole Transport Layer by Organic Monomolecular Strategy for Efficient Inverted Perovskite Solar Cells. Solar Rrl, 2020, 4, 2000011.	5.8	6
53	How a trapeziform flake of monolayer WS2 formed on SiO2(1Â0Â0)? A first-principle study. Applied Surface Science, 2020, 517, 145864.	6.1	2
54	Bifunctional Ultrathin PCBM Enables Passivated Trap States and Cascaded Energy Level toward Efficient Inverted Perovskite Solar Cells. ACS Applied Materials & Interfaces, 2020, 12, 20103-20109.	8.0	35

#	Article	IF	CITATIONS
55	Towards Simplifying the Device Structure of Highâ€Performance Perovskite Solar Cells. Advanced Functional Materials, 2020, 30, 2000863.	14.9	67
56	Polyoxometalates as electron and proton reservoir assist electrochemical CO2 reduction. APL Materials, 2020, 8, .	5.1	23
57	Polyoxometalateâ€Derived Hexagonal Molybdenum Nitrides (MXenes) Supported by Boron, Nitrogen Codoped Carbon Nanotubes for Efficient Electrochemical Hydrogen Evolution from Seawater. Advanced Functional Materials, 2019, 29, 1805893.	14.9	69
58	Synergistic effects of multiple functional ionic liquid-treated PEDOT:PSS and less-ion-defects S-acetylthiocholine chloride-passivated perovskite surface enabling stable and hysteresis-free inverted perovskite solar cells with conversion efficiency over 20%. Nano Energy, 2019, 63, 103866.	16.0	60
59	Free-Molecular-Flow Modulated Synthesis of Hexagonal Boron Nitride Monolayers. Crystal Growth and Design, 2019, 19, 7007-7014.	3.0	10
60	Single-electrode triboelectric nanogenerator based on economical graphite coated paper for harvesting waste environmental energy. Nano Energy, 2019, 66, 104141.	16.0	71
61	Synthesis, optimization and applications of ZnO/polymer nanocomposites. Materials Science and Engineering C, 2019, 98, 1210-1240.	7.3	191
62	Joule heating driven infrared switching in flexible VO <sub>2</sub> nanoparticle films with reduced energy consumption for smart windows. Journal of Materials Chemistry A, 2019, 7, 4516-4524.	10.3	44
63	Liberating Researchers from the Glovebox: A Universal Thermal Radiation Protocol Toward Efficient Fully Airâ€Processed Perovskite Solar Cells. Solar Rrl, 2019, 3, 1800324.	5.8	21
64	Organic Monomolecular Layers Enable Energy-Level Matching for Efficient Hole Transporting Layer Free Inverted Perovskite Solar Cells. ACS Nano, 2019, 13, 1625-1634.	14.6	41
65	One-pot facile simultaneous <i>in situ</i> synthesis of conductive Ag–polyaniline composites using Keggin and Preyssler-type phosphotungstates. RSC Advances, 2019, 9, 2772-2783.	3.6	9
66	Vanadium self-intercalated C/V1.11S2 nanosheets with abundant active sites for enhanced electro-catalytic hydrogen evolution. Electrochimica Acta, 2019, 300, 208-216.	5.2	19
67	Theoretical investigating of graphene/antimonene heterostructure as a promising high cycle capability anodes for fast-charging lithium ion batteries. Applied Surface Science, 2019, 491, 451-459.	6.1	33
68	Enhanced stability and photovoltage for inverted perovskite solar cells <i>via</i> precursor engineering. Journal of Materials Chemistry A, 2019, 7, 15880-15886.	10.3	22
69	Actuators: Singleâ€Crystalline Vanadium Dioxide Actuators (Adv. Funct. Mater. 20/2019). Advanced Functional Materials, 2019, 29, 1970138.	14.9	0
70	MOFs-derived ZnCo–Fe core–shell nanocages with remarkable oxygen evolution reaction performance. Journal of Materials Chemistry A, 2019, 7, 17299-17305.	10.3	47
71	Singleâ€Crystalline Vanadium Dioxide Actuators. Advanced Functional Materials, 2019, 29, 1900527.	14.9	37
72	Oil boundary approach for sublimation enabled camphor mediated graphene transfer. Journal of Colloid and Interface Science, 2019, 546, 11-19.	9.4	13

#	Article	IF	CITATIONS
73	Binary organic spacer-based quasi-two-dimensional perovskites with preferable vertical orientation and efficient charge transport for high-performance planar solar cells. Journal of Materials Chemistry A, 2019, 7, 9542-9549.	10.3	50
74	A Universal Stamping Method of Graphene Transfer for Conducting Flexible and Transparent Polymers. Scientific Reports, 2019, 9, 3999.	3.3	31
75	Nature inspired ZnO/ZnS nanobranch-like composites, decorated with Cu(OH)2 clusters for enhanced visible-light photocatalytic hydrogen evolution. Applied Catalysis B: Environmental, 2019, 253, 379-390.	20.2	90
76	Recent advances in fabrication strategies, phase transition modulation, and advanced applications of vanadium dioxide. Applied Physics Reviews, 2019, 6, .	11.3	93
77	Improvement on the performance of perovskite solar cells by doctor-blade coating under ambient condition with hole-transporting material optimization. Journal of Energy Chemistry, 2019, 38, 207-213.	12.9	27
78	Electrocatalytic Hydrogen Production: Polyoxometalateâ€Derived Hexagonal Molybdenum Nitrides (MXenes) Supported by Boron, Nitrogen Codoped Carbon Nanotubes for Efficient Electrochemical Hydrogen Evolution from Seawater (Adv. Funct. Mater. 8/2019). Advanced Functional Materials, 2019, 29, 1970046.	14.9	28
79	Intrinsic valley Hall transport in atomically thin MoS2. Nature Communications, 2019, 10, 611.	12.8	77
80	Carbon Nanotubes with Carbon Blacks as Cofillers to Improve Conductivity and Stability. ACS Omega, 2019, 4, 4169-4175.	3.5	15
81	Easily Synthesized Polyaniline@Cellulose Nanowhiskers Better Tune Network Structures in Ag-Based Adhesives: Examining the Improvements in Conductivity, Stability, and Flexibility. Nanomaterials, 2019, 9, 1542.	4.1	10
82	Phase-transition modulated, high-performance dual-mode photodetectors based on WSe <sub>2</sub> /VO <sub>2</sub> heterojunctions. Applied Physics Reviews, 2019, 6, 041407.	11.3	50
83	Excellent self-healing and antifogging coatings based on polyvinyl alcohol/hydrolyzed poly(styrene-co-maleic anhydride). Journal of Materials Science, 2019, 54, 5961-5970.	3.7	27
84	Elastic Properties and Fracture Behaviors of Biaxially Deformed, Polymorphic MoTe <sub>2</sub> . Nano Letters, 2019, 19, 761-769.	9.1	67
85	Hole-transporting layer based on a conjugated polyelectrolyte with organic cations enables efficient inverted perovskite solar cells. Nano Energy, 2019, 57, 248-255.	16.0	52
86	A New Effective Approach to Prevent the Degradation of Black Phosphorus: The Scandium Transition Metal Doping. Journal of Physical Chemistry C, 2018, 122, 9654-9662.	3.1	20
87	Thermally Sensitive Nâ€Type Thermoelectric Aniline Oligomerâ€Blockâ€Polyethylene Glycolâ€Blockâ€Aniline Oligomer ABA Triblock Copolymers. Macromolecular Chemistry and Physics, 2018, 219, 1700635.	2.2	6
88	Electronically semitransparent ZnO nanorods with superior electron transport ability for DSSCs and solar photocatalysis. Ceramics International, 2018, 44, 7202-7208.	4.8	33
89	Fabricating Highâ€Efficient Bladeâ€Coated Perovskite Solar Cells under Ambient Condition Using Lead Acetate Trihydrate. Solar Rrl, 2018, 2, 1700214.	5.8	29
90	Twin Defect Derived Growth of Atomically Thin MoS <sub>2</sub> Dendrites. ACS Nano, 2018, 12, 635-643.	14.6	92

#	Article	IF	CITATIONS
91	Proton Conducting Polyoxometalate/Polypyrrole Films and Their Humidity Sensing Performance. ACS Applied Nano Materials, 2018, 1, 564-571.	5.0	32
92	Crystallization manipulation and morphology evolution for highly efficient perovskite solar cell fabrication <i>via</i> hydration water induced intermediate phase formation under heat assisted spin-coating. Journal of Materials Chemistry A, 2018, 6, 3012-3021.	10.3	40
93	PEDOT:PSS/graphene quantum dots films with enhanced thermoelectric properties via strong interfacial interaction and phase separation. Scientific Reports, 2018, 8, 6441.	3.3	151
94	A new numerical method for delay and advanced integro-differential equations. Numerical Algorithms, 2018, 77, 381-412.	1.9	6
95	Superhigh strength of geopolymer with the addition of polyphosphate. Ceramics International, 2018, 44, 2578-2583.	4.8	20
96	Gate-tunable strong-weak localization transition in few-layer black phosphorus. Nanotechnology, 2018, 29, 035204.	2.6	10
97	Natural phosphate-supported Cu( <scp>ii</scp> ), an efficient and recyclable catalyst for the synthesis of xanthene and 1,4-disubstituted-1,2,3-triazole derivatives. RSC Advances, 2018, 8, 41536-41547.	3.6	23
98	Polymer Assisted Small Molecule Hole Transport Layers Toward Highly Efficient Inverted Perovskite Solar Cells (Solar RRL 11â^•2018). Solar Rrl, 2018, 2, 1870228.	5.8	0
99	Direct <i>Z</i> -Scheme Cs <sub>2</sub> O–Bi <sub>2</sub> O <sub>3</sub> –ZnO Heterostructures as Efficient Sunlight-Driven Photocatalysts. ACS Omega, 2018, 3, 12260-12269.	3.5	60
100	Strain-Enhanced Li Storage and Diffusion on the Graphyne as the Anode Material in the Li-Ion Battery. Journal of Physical Chemistry C, 2018, 122, 22838-22848.	3.1	58
101	Effect of sintering temperature on structural, electrical, and ferroelectric properties of lanthanum and sodium co-substituted barium titanate ceramics. Journal of Alloys and Compounds, 2018, 762, 49-61.	5.5	35
102	Fluctuation-induced tunneling conduction in iodine-doped bilayer graphene. Journal of Applied Physics, 2018, 123, 244302.	2.5	2
103	Surface modification and grafting of carbon fibers: A route to better interface. Progress in Crystal Growth and Characterization of Materials, 2018, 64, 75-101.	4.0	59
104	Directly Probing Light Absorption Enhancement of Single Hierarchical Structures with Engineered Surface Roughness. Scientific Reports, 2018, 8, 12283.	3.3	6
105	Polymer Assisted Small Molecule Hole Transport Layers Toward Highly Efficient Inverted Perovskite Solar Cells. Solar Rrl, 2018, 2, 1800173.	5.8	30
106	Intensive Exposure of Functional Rings of a Polymeric Holeâ€Transporting Material Enables Efficient Perovskite Solar Cells. Advanced Materials, 2018, 30, e1804028.	21.0	104
107	Efficiency and stability enhancement of perovskite solar cells by introducing CsPbI3 quantum dots as an interface engineering layer. NPG Asia Materials, 2018, 10, 552-561.	7.9	115
108	Improving the Performance of PbS Quantum Dot Solar Cells by Optimizing ZnO Window Layer. Nano-Micro Letters, 2017, 9, 24.	27.0	50

#	Article	IF	CITATIONS
109	Efficient and Stable Perovskite Solar Cells Prepared in Ambient Air Based on Surface-Modified Perovskite Layer. Journal of Physical Chemistry C, 2017, 121, 6546-6553.	3.1	84
110	Simultaneous determination of epinephrine, ascorbic acid and folic acid using TX-100 modified carbon paste electrode: A cyclic voltammetric study. Journal of Molecular Liquids, 2017, 231, 379-385.	4.9	36
111	Phosphorous doped graphitic-C3N4 hierarchical architecture for hydrogen production from water under visible light. Materials Today Energy, 2017, 5, 91-98.	4.7	27
112	Functional Nanomaterials for Transparent Electrodes. Springer Series on Polymer and Composite Materials, 2017, , 345-376.	0.7	0
113	Shape-Dependent Defect Structures of Monolayer MoS <sub>2</sub> Crystals Grown by Chemical Vapor Deposition. ACS Applied Materials & Interfaces, 2017, 9, 763-770.	8.0	45
114	Influence of High Dose Gamma Irradiation on Electrical Characteristics of Si Photo Detectors. ECS Journal of Solid State Science and Technology, 2017, 6, Q132-Q135.	1.8	5
115	Study of the mobility activation in ZnSe thin films deposited using inert gas condensation. Journal of Science: Advanced Materials and Devices, 2017, 2, 432-436.	3.1	5
116	Axial Modulation of Metal–Insulator Phase Transition of VO <sub>2</sub> Nanowires by Graded Doping Engineering for Optically Readable Thermometers. Journal of Physical Chemistry C, 2017, 121, 24877-24885.	3.1	31
117	A laser irradiation synthesis of strongly-coupled VOx-reduced graphene oxide composites as enhanced performance supercapacitor electrodes. Materials Today Energy, 2017, 5, 222-229.	4.7	13
118	Low-temperature-processed SnO <sub>2</sub> –Cl for efficient PbS quantum-dot solar cells via defect passivation. Journal of Materials Chemistry A, 2017, 5, 17240-17247.	10.3	63
119	Efficient coupling of a hierarchical V <sub>2</sub> O <sub>5</sub> @Ni <sub>3</sub> S <sub>2</sub> hybrid nanoarray for pseudocapacitors and hydrogen production. Journal of Materials Chemistry A, 2017, 5, 17954-17962.	10.3	88
120	Ambipolar quantum transport in few-layer black phosphorus. Physical Review B, 2017, 96, .	3.2	26
121	Heterogeneous growth mechanism of ZnO nanostructures and the effects of their morphology on optical and photocatalytic properties. CrystEngComm, 2017, 19, 3299-3312.	2.6	86
122	Three Dimensional Sculpturing of Vertical Nanowire Arrays by Conventional Photolithography. Scientific Reports, 2016, 6, 18886.	3.3	7
123	Y-shaped ZnO Nanobelts Driven from Twinned Dislocations. Scientific Reports, 2016, 6, 22494.	3.3	10
124	Negative compressibility in graphene-terminated black phosphorus heterostructures. Physical Review B, 2016, 93, .	3.2	10
125	V2O5-C-SnO2 Hybrid Nanobelts as High Performance Anodes for Lithium-ion Batteries. Scientific Reports, 2016, 6, 33597.	3.3	31
126	Universal low-temperature Ohmic contacts for quantum transport in transition metal dichalcogenides. 2D Materials, 2016, 3, 021007.	4.4	102

7	#	Article	IF	CITATIONS
-	127	A fast transfer-free synthesis of high-quality monolayer graphene on insulating substrates by a simple rapid thermal treatment. Nanoscale, 2016, 8, 2594-2600.	5.6	20
3	128	Directly Metering Light Absorption and Heat Transfer in Single Nanowires Using Metal–Insulator Transition in VO <sub>2</sub> . Advanced Optical Materials, 2015, 3, 336-341.	7.3	21
-	129	Hierarchical ZnO Nanostructures with Blooming Flowers Driven by Screw Dislocations. Scientific Reports, 2015, 5, 8226.	3.3	14
]	130	Nanoscale variation in energy dissipation in austenitic shape memory alloys in ultimate loading cycles. Journal of Intelligent Material Systems and Structures, 2015, 26, 2411-2417.	2.5	2
	131	Powerful, Multifunctional Torsional Micromuscles Activated by Phase Transition. Advanced Materials, 2014, 26, 1746-1750.	21.0	76
1	132	Enhanced photocatalytic performance of TiO2-ZnO hybrid nanostructures. Scientific Reports, 2014, 4, 4181.	3.3	248
	133	Self-Assembly and Horizontal Orientation Growth of VO2 Nanowires. Scientific Reports, 2014, 4, 5456.	3.3	49
1	134	Tuning the optical and electrical properties of hydrothermally grown ZnO nanowires by sealed post annealing treatment. Solid State Communications, 2013, 160, 41-46.	1.9	12
	135	Transcription Initiation Factor IIB Involves in Schwann Cell Differentiation after Rat Sciatic Nerve Crush. Journal of Molecular Neuroscience, 2013, 49, 491-498.	2.3	5
-	136	Dynamically Tracking the Strain Across the Metal–Insulator Transition in VO <sub>2</sub> Measured Using Electromechanical Resonators. Nano Letters, 2013, 13, 4685-4689.	9.1	16
-	137	Temperature variations at nano-scale level in phase transformed nanocrystalline NiTi shape memory alloys adjacent to graphene layers. Nanoscale, 2013, 5, 6479.	5.6	12
-	138	Axially Engineered Metal–Insulator Phase Transition by Graded Doping VO <sub>2</sub> Nanowires. Journal of the American Chemical Society, 2013, 135, 4850-4855.	13.7	96
-	139	Comprehensive study of the metal-insulator transition in pulsed laser deposited epitaxial VO2 thin films. Journal of Applied Physics, 2013, 113, .	2.5	134
	140	Effect of graphene layers on the thermomechanical behaviour of a NiTi shape memory alloy during the nanoscale phase transition. Scripta Materialia, 2013, 68, 420-423.	5.2	14
-	141	Combinational rate effects on the performance of nano-grained pseudoelastic Nitinols. Materials Letters, 2013, 105, 98-101.	2.6	9
-	142	Performance Limits of Microactuation with Vanadium Dioxide as a Solid Engine. ACS Nano, 2013, 7, 2266-2272.	14.6	66
1	143	<font>Ni</font> –NTA-COATED NANOWIRE MATERIALS FOR PROTEIN ENRICHMENT AND THE APPLICATION IN A MEDICAL DEVICE USED FOR BLOOD GLUCOSE DEGRADATION. Nano, 2013, 08, 1350029.	1.0	3
-	144	Phase Transformation Evolution in NiTi Shape Memory Alloy under Cyclic Nanoindentation Loadings at Dissimilar Rates. Scientific Reports, 2013, 3, 3412.	3.3	17

#	Article	IF	CITATIONS
145	Nature of hardness evolution in nanocrystalline NiTi shape memory alloys during solid-state phase transition. Scientific Reports, 2013, 3, 2476.	3.3	14
146	Correlation between the Morphology and Performance Enhancement of ZnO Hierarchical Flower Photoanodes in Quasi-Solid Dye-Sensitized Solar Cells. Journal of Nanomaterials, 2012, 2012, 1-8.	2.7	3
147	Ultra-long, free-standing, single-crystalline vanadium dioxide micro/nanowires grown by simple thermal evaporation. Applied Physics Letters, 2012, 100, .	3.3	103
148	Directed assembly of nano-scale phase variants in highly strained BiFeO3 thin films. Journal of Applied Physics, 2012, 112, 064102.	2.5	35
149	Giant-Amplitude, High-Work Density Microactuators with Phase Transition Activated Nanolayer Bimorphs. Nano Letters, 2012, 12, 6302-6308.	9.1	158
150	Dense Electron System from Gate-Controlled Surface Metal–Insulator Transition. Nano Letters, 2012, 12, 6272-6277.	9.1	57
151	Optimizing nanosheet-based ZnO hierarchical structure through ultrasonic-assisted precipitation for remarkable photovoltaic enhancement in quasi-solid dye-sensitized solar cells. Journal of Materials Chemistry, 2012, 22, 13097.	6.7	48
152	ZnO hierarchical structures for efficient quasi-solid dye-sensitized solar cells. Physical Chemistry Chemical Physics, 2011, 13, 10631.	2.8	39
153	Zn <sub>2</sub> TiO <sub>4</sub> â^'ZnO Nanowire Axial Heterostructures Formed by Unilateral Diffusion. Journal of Physical Chemistry C, 2011, 115, 78-82.	3.1	18
154	Controllable Fabrication of Three-Dimensional Radial ZnO Nanowire/Silicon Microrod Hybrid Architectures. Crystal Growth and Design, 2011, 11, 147-153.	3.0	52
155	Heat Transfer across the Interface between Nanoscale Solids and Gas. ACS Nano, 2011, 5, 10102-10107.	14.6	63
156	Carbon-assisted nucleation and vertical growth of high-quality ZnO nanowire arrays. AIP Advances, 2011, 1, 032104.	1.3	8
157	Fabrication and Structure Characterization of Te Butterfly Nanostructures. Journal of Nanoscience and Nanotechnology, 2011, 11, 11037-11040.	0.9	0
158	Elevated expression of CAPON and neuronal nitric oxide synthase in the sciatic nerve of rats following constriction injury. Veterinary Journal, 2011, 187, 374-380.	1.7	8
159	A self-entanglement mechanism for continuous pulling of carbon nanotube yarns. Carbon, 2011, 49, 4996-5001.	10.3	39
160	Tailoring the luminescence emission of ZnO nanostructures by hydrothermal post-treatment in water. Applied Physics Letters, 2010, 96, 223105.	3.3	35
161	Carbon-assisted growth technology for ZnO nanowires. , 2010, , .		1
162	Vertically aligned ZnO/amorphous-Si core–shell heterostructured nanowire arrays. Nanotechnology, 2010, 21, 475703.	2.6	23

#	Article	IF	CITATIONS
163	Nanostructural Transformation and Formation of Heterojunctions from Si Nanowires. ACS Nano, 2010, 4, 5559-5564.	14.6	9
164	Fabrication and structure characterization of Te butterfly nanostructures. , 2010, , .		0
165	Photoluminescence study of single ZnO nanostructures: Size effect. Applied Physics Letters, 2009, 95, 053113.	3.3	20
166	High-Quality ZnO Nanowire Arrays Directly Fabricated from Photoresists. ACS Nano, 2009, 3, 53-58.	14.6	74
167	Growth and Photocatalytic Activity of Dendrite-like ZnO@Ag Heterostructure Nanocrystals. Crystal Growth and Design, 2009, 9, 3278-3285.	3.0	206
168	Involvement of CAPON and Nitric Oxide Synthases in Rat Muscle Regeneration After Peripheral Nerve Injury. Journal of Molecular Neuroscience, 2008, 34, 89-100.	2.3	26
169	Chemical Stability of ZnO Nanostructures in Simulated Physiological Environments and Its Application in Determining Polar Directions. Inorganic Chemistry, 2008, 47, 7868-7873.	4.0	24
170	Spatially resolved photoluminescence study of single ZnO tetrapods. Nanotechnology, 2008, 19, 405702.	2.6	10
171	Site-Specific Deposition of Titanium Oxide on Zinc Oxide Nanorods. Journal of Physical Chemistry C, 2007, 111, 16712-16716.	3.1	24
172	Controllable growth of zinc oxide micro- and nanocrystals by oxidization of Zn–Cu alloy. Journal of Solid State Chemistry, 2005, 178, 819-824.	2.9	6
173	Growth of boron nitride nanotube film in situ. Applied Physics A: Materials Science and Processing, 2005, 81, 527-529.	2.3	18
174	Metal Oxide Coating on Carbon Nanotubes by a Methanol-Thermal Method. Journal of Nanoscience and Nanotechnology, 2005, 5, 932-936.	0.9	6
175	Preparation of aluminum borate nanowires. Journal of Crystal Growth, 2004, 263, 600-604.	1.5	35
176	Synthesis of gallium borate nanowires. Journal of Crystal Growth, 2004, 263, 504-509.	1.5	12
177	Catalytic synthesis of aluminum borate nanowires. Chemical Physics Letters, 2003, 373, 626-629.	2.6	37
178	Heat Transfer Enhancement of n-Type Organic Semiconductors by an Insulator Blend Approach. ACS Applied Materials & Interfaces, 0, , .	8.0	1